7

# Modeling of Sediment Transport in Surface Flow with a Grass Strip

Takahiro Shiono[1] and Kuniaki Miyamoto[2]
[1]*National Institute for Rural Engineering, NARO*
[2]*Graduate School of Life and Environmental Sciences*
*University of Tsukuba*
*Japan*

## 1. Introduction

Reddish sediment runoff from land areas during rainfall causes environmental problems in coastal areas of the Okinawa region, Japan. Sediment delivered to the coastal areas causes water pollution, sedimentation and degrades the coastal ecosystems and fisheries resources. Agricultural fields are a major source of sediment runoff in the region (Yoshinaga & Onaga, 1993; Minami et al., 2002). Nakasonoe et al. (1998) reported that sediment from agricultural fields accounts for 70% of the total sediment runoff in the region. Countermeasures for runoff in agricultural fields are promoted as an important issue in the Okinawa region.

Countermeasures so far proposed include terrace work, drainage canals, sediment ponds, grass strips, cover cropping, mulch farming, contour farming, deep tillage, crop rotation and green manure (Hudson, 1995; Morgan, 1995). The grass strip countermeasure involves installing grass bands at the downstream end of an agricultural field to reduce the amount of non-point source pollutants, such as sediment and nutrients from an agricultural field into the stream (Dillaha et al., 1989). Grass strips are currently installed by prefectural governments assisted by the Ministry of Agriculture, Forestry and Fisheries as public work projects for water conservation, and also as a measure to help conserve agricultural land, water and the environment in rural areas. Grass strips can also be installed by farmers themselves as one of agricultural activities.

There are various factors affecting how effectively grass strips reduce sediment runoff, such as flow rate of inflowing water, sediment properties, slope conditions and features of the grass (Haan et al., 1994). When installing grass strips as a countermeasure for sediment runoff, various conditions must be taken into consideration. In designing grass strips, it is necessary to know the quantitative relationships between the various factors influencing grass strips and their effects on reduction of sediment runoff, and to determine appropriate and reasonable parameters for installing grass strips.

In previous studies, Sugawara et al. (2001), Osawa et al. (2005) and Shiono et al. (2005) conducted field experiments in Ishigaki Island and the northern part of the Okinawa Main Island, and reported their results on the effects of grass strips for reducing reddish sediment runoff. Shiono et al. (2007) also reported the influence that the length of grass strips in the direction of flow and particle sizes of sediment flowing into grass strips have on the ability of grass strips to reduce reddish sediment runoff. These results were obtained from field experiments conducted in the northern part of the Okinawa Main Island. However, since the effects that grass strips have on reducing reddish sediment runoff presented in these studies were obtained under limited conditions, these effects do not fully reveal the relationship between various installation conditions of grass strips conceivable at a site and their effects on reducing the runoff of reddish sediment.

Therefore, this study aims to establish a mathematical model to represent the sediment trapping process of grass strips as part of efforts to present, through the analysis of a mathematical model, the relationship between various installation conditions of grass strips and their effects on reducing the runoff of reddish sediment. First, flume experiments were performed using a simulated grass model and then a grass model developed to experimentally simulate the sediment-trapping process of grass strips. The results of these experiments allowed us to obtain the necessary characteristics. Next, a mathematical model was established for simulating the sediment trapping processes of the grass strips used in the flume experiments, and the model was verified.

## 2. Flume experiment

### 2.1 Flume experiment with bamboo rod model

Flume experiments with a bamboo rod model simulating grass strips were conducted to clarify the process of surface flow and sediment transport in and around a grass strip. The experiments used an acrylic flume with a rectangular cross section, total length 12.0 m, width 0.145 m, depth 0.150 m and gradient of 0.02. The rod model was made of a polyvinyl chloride plate with a width of 0.145 m and thickness of 3 mm, where 2.5 mm-diameter and 0.15 m-long bamboo rods were arranged vertically to form grids of 40,000 rods/$m^2$. The rod model was installed as a section extending 1.50 m from the downstream end of the flume. To prevent the occurrence of steps on the flume floor when installing this model, a plywood board with a thickness of 9 mm was placed on the flume floor immediately under the model, and another board with a thickness of 12 mm placed upstream of the model. Both boards were coated with varnish.

Four types of sediment were used for the experiments: GK-9, NK-9, Goto Clay (these three were made by Kumamoto Silicasand Industry Co., Ltd.) and Kunigami Maji. The last soil was collected from the Arashiyama field in Nago on the northern part of the Okinawa Main Island (26˚38'N, 127˚59.5'E). The particle densities of GK-9, NK-9, Goto Clay and Kunigami Maji were 2.63, 2.61, 2.71 and 2.71 Mg/$m^3$, respectively. Figure 1 shows the particle size distribution of the test sediments used.

Figure 2 shows an outline of the flume experiment with the rod model, and Table 1 shows the experimental conditions. In these experiments, clean water with a constant flow rate was supplied from the upstream end of the flume. Then, a sediment-water mixture was supplied at a constant rate into the running water at a point 2.0 m downstream from the upstream end, so that sediment-laden water with a constant concentration of sediment flowed at a constant rate. The flow rate was set to form a surpercritical flow so as to prevent sediment from being deposited upstream of the flume. The flow rate was measured by means of an HS flume installed at the downstream end. The sediment-water mixture was prepared in advance in a bucket, which was mixed with a mixer during the experiments. The flow rate of the mixture supplied was regulated using a meter pump (Masterflex Inc, 7523-60). The experiments continued for durations of 150 to 390 minutes. While the water was running, water levels were measured at intervals of 0.2 to 0.5 m along the length of the flume with a point gage (KENEK, PH-340) to determine the water surface profile. Two hundred ml of water was sampled from the running water both upstream and downstream of the rod model every 30 minutes and sediment concentrations in the running water measured by the oven-drying method. The upstream sampling point was set immediately upstream of the hydraulic jump due to the influence of the rod model. After each experiment, the bed surface profile was measured along the length of the flume with the point gage.

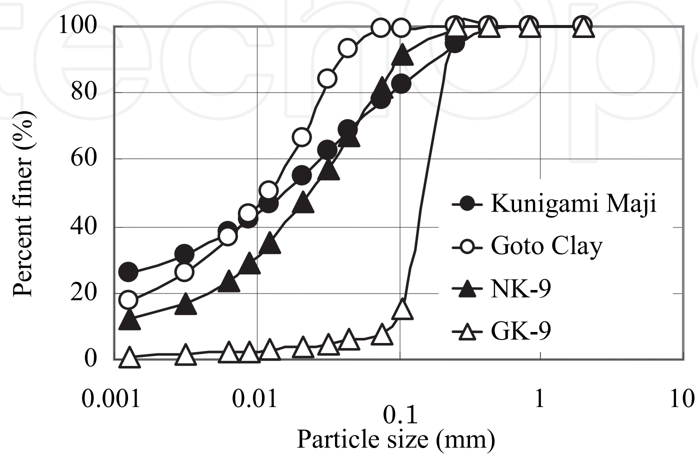


Fig. 1. Particle size distribution of test sediments

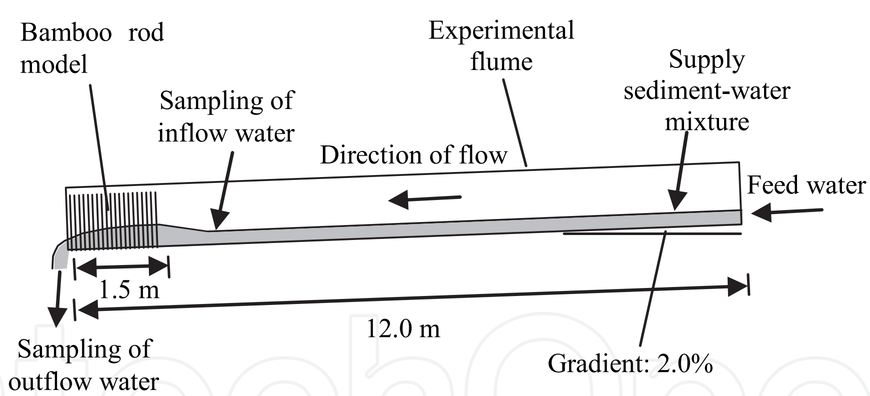


Fig. 2. Outline of flume experiment with a bamboo rod model

### 2.2 Flume experiment with grass model

Flume experiments with a grass model simulating grass strips were also conducted to clarify the characteristics of sediment removal by grass strips. Centipede grass (*Eremochloa ophiuroides* (Munro) Hack.), a turf grass, was used for the grass model. Shiono et al. (2007) reported that grass strips made from centipede grass were effective for reducing reddish sediment loads under typical farmland conditions. Dead grass was substituted for living grass in these experiments because the shape and the stiffness of the dead grass was almost the same as the living grass and multiple flume experiments could be conducted under the same grass conditions. The turf grass was grown at a field in the National Agricultural

Research Center for Kyushu Okinawa Region in Kumamoto, Japan. When collected, the grass was 10 cm high, the vegetation cover ratio was 100% and the surface portion was dead. The grass bodies collected also covered the root section from the surface down to a depth of 10 cm with soil attached. After collection, only the surface portion was selected, and the roots and soil were removed. These plant bodies were then attached to a polyvinyl chloride plate with a width of 0.145 m and thickness of 3 mm to form the grass model used for the experiments.

| Case | Sediment | Flow rate $Q$ ($m^3 \cdot s^{-1}$) | Water flowing time (min) | Water depth on upstream side $h_0$ (mm) | Froude number $Fr_0$ | Average sediment concentration on upstream side $C_{in}$ ($m^3 \cdot m^{-3}$) | Average sediment concentration on downstream side $C_{out}$ ($m^3 \cdot m^{-3}$) | Sediment reduction rate (%) |
|---|---|---|---|---|---|---|---|---|
| A-1 | GK-9 | $2.07\times10^{-4}$ | 285 | 4.33 | 1.60 | $5.93\times10^{-4}$ | $1.41\times10^{-5}$ | 97.6 |
| A-2 | NK-9 | $2.02\times10^{-4}$ | 285 | 3.59 | 2.07 | $9.89\times10^{-4}$ | $3.91\times10^{-4}$ | 60.5 |
| A-3 | NK-9 | $2.13\times10^{-4}$ | 205 | 4.69 | 1.46 | $2.26\times10^{-3}$ | $8.47\times10^{-4}$ | 62.5 |
| A-4 | NK-9 | $1.03\times10^{-4}$ | 390 | 3.38 | 1.15 | $8.43\times10^{-4}$ | $3.28\times10^{-4}$ | 61.1 |
| A-5 | NK-9 | $1.10\times10^{-4}$ | 390 | 3.06 | 1.43 | $4.75\times10^{-4}$ | $9.96\times10^{-5}$ | 79.0 |
| A-6 | Goto Clay | $2.07\times10^{-4}$ | 390 | 4.34 | 1.60 | $1.07\times10^{-3}$ | $6.33\times10^{-4}$ | 40.8 |
| A-7 | Goto Clay | $2.02\times10^{-4}$ | 195 | 4.73 | 1.37 | $2.66\times10^{-3}$ | $1.50\times10^{-3}$ | 43.6 |
| A-8 | Goto Clay | $1.07\times10^{-4}$ | 390 | 3.47 | 1.16 | $1.13\times10^{-3}$ | $4.89\times10^{-4}$ | 56.7 |
| A-9 | Goto Clay | $1.10\times10^{-4}$ | 375 | 3.23 | 1.32 | $4.59\times10^{-4}$ | $1.66\times10^{-4}$ | 63.8 |
| A-10 | Kunigami Maji | $2.07\times10^{-4}$ | 270 | 5.09 | 1.26 | $1.68\times10^{-3}$ | $7.52\times10^{-4}$ | 55.2 |
| A-11 | Kunigami Maji | $1.10\times10^{-4}$ | 240 | 3.41 | 1.22 | $9.15\times10^{-4}$ | $4.19\times10^{-4}$ | 54.2 |
| A-12 | Kunigami Maji | $3.04\times10^{-4}$ | 150 | 5.50 | 1.64 | $1.55\times10^{-3}$ | $3.96\times10^{-4}$ | 74.4 |

Table 1. Summary of experimental conditions and results

The flume and grass models were installed in the same way as in 2.1, and the above-mentioned Kunigami Maji sediment was used in the experiments. The experiments were conducted in a manner similar to that in 2.1, that is, clean water was supplied from the upstream end of the flume. Then at a point 2.0 m downstream from the upstream end, a sediment-water mixture was supplied into the running water, so that sediment-laden water with a constant concentration of sediment flowed at a constant rate. Each experiment continued for 60 minutes. While the water was running, water level was measured for the water surface profile along the length of the flume as in 2.1. Also water was sampled every 10 minutes to determine the sediment concentration in the upstream and downstream flow of the grass model. The experimental conditions are given in Table 2. In Cases B-1 to B-6, the length of the model in the longitudinal direction was fixed at 1.5 m, while the flow rate was set at three steps within the range of $1.01\times10^{-4}$ to $2.95\times10^{-4}$ $m^3 \cdot s^{-1}$ and the sediment concentration was set at two steps of $7\times10^{-4}$ and $1.4\times10^{-3}$ $m^3 \cdot m^{-3}$. On the other hand, in Cases C-1 to C-4, the experiments were performed with the model length set at four steps within the range of 0.5 to 5.9 m. The experiments also included sampling of running water in the upstream and downstream flows of the grass model to determine the distribution of equivalent sizes of sediment particles contained in the running water. The distribution of equivalent particle size was obtained by the pipette method. The equivalent particle size is defined here as the diameter of a spherical particle having a sediment particle density and a falling velocity that are equal to the target sediment particles or aggregates under consideration. For this purpose, only distilled water was used for dispersion of the sediment samples in the process of the pipette method.

| Case | Model length (m) | Flow rate $Q$ ($m^3 \cdot s^{-1}$) | Water flowing time (min) | Water depth on upstream side $h_0$ (mm) | Froude number $Fr_0$ | Average sediment concentration on upstream side $C_{in}$ ($m^3 \cdot m^{-3}$) | Average sediment concentration on downstream side $C_{out}$ ($m^3 \cdot m^{-3}$) | Sediment reduction rate (%) |
|---|---|---|---|---|---|---|---|---|
| B-1 | 1.5 | $1.01\times10^{-4}$ | 60 | 2.39 | 1.96 | $1.48\times10^{-3}$ | $4.65\times10^{-4}$ | 68.6 |
| B-2 | 1.5 | $1.01\times10^{-4}$ | 60 | 2.39 | 1.96 | $6.16\times10^{-4}$ | $1.47\times10^{-4}$ | 76.1 |
| B-3 | 1.5 | $1.98\times10^{-4}$ | 60 | 4.04 | 1.70 | $1.13\times10^{-3}$ | $5.35\times10^{-4}$ | 52.7 |
| B-4 | 1.5 | $1.98\times10^{-4}$ | 60 | 4.04 | 1.70 | $5.20\times10^{-4}$ | $1.93\times10^{-4}$ | 62.9 |
| B-5 | 1.5 | $2.95\times10^{-4}$ | 60 | 4.80 | 1.97 | $1.53\times10^{-3}$ | $7.75\times10^{-4}$ | 49.3 |
| B-6 | 1.5 | $2.95\times10^{-4}$ | 60 | 4.80 | 1.97 | $7.82\times10^{-4}$ | $3.45\times10^{-4}$ | 55.9 |
| C-1 | 0.5 | $1.98\times10^{-4}$ | 60 | 3.89 | 1.80 | $1.35\times10^{-3}$ | $7.27\times10^{-4}$ | 46.1 |
| C-2 | 1.5 | $1.98\times10^{-4}$ | 60 | 3.86 | 1.82 | $1.50\times10^{-3}$ | $6.64\times10^{-4}$ | 55.7 |
| C-3 | 3.1 | $1.98\times10^{-4}$ | 60 | 3.95 | 1.76 | $1.45\times10^{-3}$ | $6.31\times10^{-4}$ | 56.5 |
| C-4 | 5.9 | $1.98\times10^{-4}$ | 60 | 3.85 | 1.83 | $1.29\times10^{-3}$ | $5.09\times10^{-4}$ | 60.5 |

Table 2. Summary of experimental conditions and result

### 2.3 Experiments on flow conditions in grass and rod models

Pipe channel experiments were performed to identify flow conditions within the grass models used in the above mentioned experiments. These experiments adopted an acrylic pipe channel with a rectangular cross section, total length 1.0 m, width 0.145 m and depth 0.10 m, where the grass model was placed along the entire channel. Then, as indicated in Fig. 3, the channel was filled with clear water at a constant flow rate to determine the relationship between the flow rate and the hydraulic gradient. The flow rate was $Q$ = $6.94\times10^{-5}$ to $2.03\times10^{-3}$ $m \cdot s^{-3}$, and the average flow velocity in the cross section $u$ = $1.45\times10^{-2}$ to $1.76\times10^{-1}$ $m \cdot s^{-1}$. The experiments provided data on the flow conditions corresponding to 9 to 15 steps within the above parameter ranges, where measurements were made using a bucket. The hydraulic gradient was obtained from the water level differences between the two acrylic pipes installed in the pipe channel and the distance (0.90 m) between them. The heights of the grass model were set at four steps: 3.2, 5.5, 7.7 and 10.0 cm. First, the experiment was conducted for the 10.0 cm-high grass model, and then the top was cut to 7.7 cm. Subsequently, other heights were also set in a similar way. For grass heights other than 10.0 cm, plywood boards were placed beneath the grass model to adjust the channel floor height and ensure that all water flowing into the channel passed through the grass.

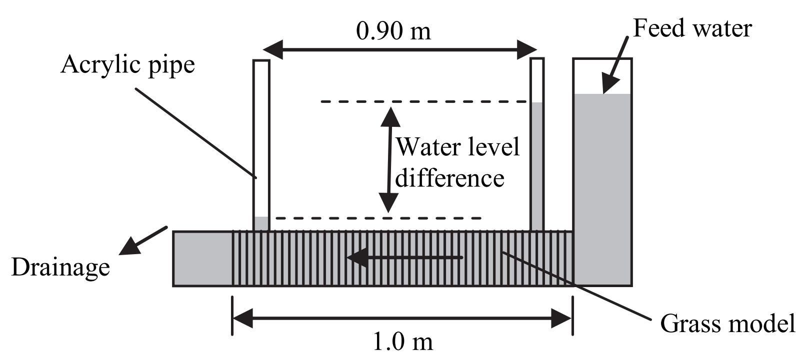


Fig. 3. Outline of experiment on flow conditions in grass

Experiments on the flow characteristics of the rod model were also performed in a similar manner, but the acrylic pipe channel used had a rectangular cross section with a total length of 1.0 m, a width of 0.145 m and a depth of 0.16 m, while the model height was set at one step only of 0.15 m. The flow rate given was $Q$ = $2.62\times10^{-4}$ to $3.18\times10^{-3}$ $m \cdot s^{-3}$, while the average flow velocity in the cross section was $u$ = $1.39\times10^{-2}$ to $1.69\times10^{-1}$ $m \cdot s^{-1}$. The experiments provided data on the flow conditions corresponding to 17 steps within the above parameter ranges.

## 3. Results and discussion for flume experiments

### 3.1 Flume experiments with bamboo rod model

In the experiments for Cases A-1 to A-12, the running water flowed upstream of the flume as a supercritical flow, resulting in the generation of a hydraulic jump upstream of the rod model. Downstream of the hydraulic jump the flow velocity decreased so the water ran at a subcritical flow. At the start of the experiments, the hydraulic jump was located 0.7 to 2.1 m upstream of the model upstream end. However, during the experiments, the jump location gradually shifted upstream due to sediment being deposited on the flume bed, and by the time the experiments were finished the location was 1.4 to 4.0 m upstream of the model upstream end.

The sediment contained in the running water did not deposit on the flume bed in the section upstream of the hydraulic jump, but instead flowed as bed load or suspended load sediment. In the section downstream of the hydraulic jump, that is, in the backwater section or the rod model section, some sediment was deposited on the flume bed due to a decrease in flow velocity, while other sediment passed with the running water through the rod model section. The depth of sediment deposited peaked in the backwater section, while the depth gradually decreased along the downstream direction in the model section. During the experiments, the sediment deposition depth and the length of the deposition section gradually increased, while the sediment concentration on the model downstream side remained almost unchanged.

As indicated in Table 1, the sediment reduction rates for the rod model obtained from the time average of sediment concentrations in the upstream and downstream flows of the model ranged from 40.8 to 97.6%. It is evident that the sediment reduction rates vary depending on the conditions set. Particularly, in experiment Case A-1 using sediment GK-9 with course particles, the rate was as high as 97.6%.

### 3.2 Flume experiments with the grass model

The sediment reduction rates for the grass model varied depending on the flow rate and concentration of sediment in the upstream side. As indicated in Table 2, the sediment reduction rates obtained from the time average of sediment concentrations in the upstream and downstream flows of the grass model for Cases B-1 to B-6 ranged from 49.3 to 76.1%. An overview of the relationship between the sediment reduction rate and measurements of the flow rate and the upstream-side sediment concentrations suggests the sediment reduction rate was smaller for increased flow rates, while the rate decreased to some extent for higher upstream sediment concentrations.

The sediment reduction rates of the grass model also varied in accordance with the model length. As indicated in Table 2, the sediment reduction rates obtained from the time average of sediment concentrations in the upstream and downstream flows of the grass model for Cases C-1 to C-4 ranged from 46.1 to 60.5%. In other words, the reduction rate was larger when model length increased.

The results of the analysis for particle sizes of the sediment collected on the upstream side of the grass model in each experiment showed that the average fractions of equivalent particle size for 0 to 0.002, 0.002 to 0.02, 0.02 to 0.2 and 0.2 to 0.5 mm were 13%, 44%, 39% and 4%, respectively. This evidences the sediment with a particle size equivalent to silt and fine sand is predominant, while the fraction of particles equivalent in size to clay and course sand is small.

The effect of the grass model on reducing sediment runoff varies depending on the equivalent particle size. Figure 4 shows the time-averaged sediment loads for each equivalent particle size class in the upstream and downstream flows of the grass model of experiment C-3. As is shown here, the sediment loads for particle size classes of 0.02 to 0.2 and 0.2 to 0.5 mm on the downstream side are remarkably small compared with those on the upstream side, while those of the 0 to 0.002 and 0.002 to 0.02 mm particle size classes on the downstream side are somewhat smaller than on the upstream side. The sediment reduction rates in all cases with an equivalent particle size of 0 to 0.002, 0.002 to 0.02, 0.02 to 0.2 and 0.2 to 0.5 mm were 0 to 68, 2 to 64, 88 to 100 and 100%, respectively. Sediment with an equivalent particle size of larger than 0.02 mm was mostly trapped by the grass model, while only some sediment with particle sizes smaller than 0.02 mm was trapped. Such characteristics of the sediment trapping by grass depending on particle sizes were also reported by Shiono et al. (2007).

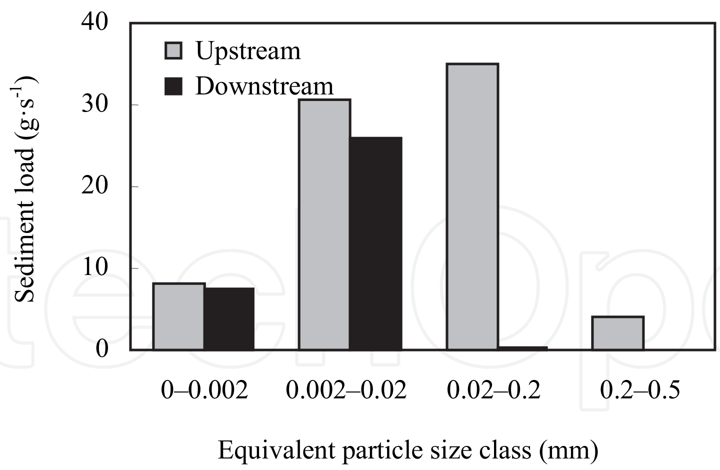


Fig. 4. Sediment load in equivalent particle size class (C-3)

### 3.3 Experiment on flow conditions in grass and rod models

Table 3 shows the values of parameters *a* and *b* of the empirical model $I = a \cdot u^b$ determined by measuring the average flow velocity in the cross section *u* ($m \cdot s^{-1}$) and the hydraulic gradient *I* obtained by the experiments on flow characteristics in the grass model and the rod model. Parameter *b* in the grass model was 1.17 to 1.32 while that in the rod model was 1.36. The above results indicate that the flows in the grass model and the rod model are in a state of transition between laminar flow and turbulent flow. If flow is turbulent the square of the velocity is proportional to the hydraulic gradient and if flow is laminar the velocity is proportional to the hydraulic gradient (Nezu and Tominaga, 2000). The above observation suggests that sediment deposited in the flume bed is less likely to be picked up as suspending sediment, because flows in the model are not in a fully developed turbulent state for flow in the model of the experiments performed in 2.1, and 2.2.

## 4. Numerical model calculation

A numerical model was constructed for simulating surface flow and sediment transport processes in and around the rod model and the grass model.

| Model type | Model height (m) | Parameter | | Coefficient of determination |
|---|---|---|---|---|
| | | *a* | *b* | |
| Grass model | 0.10 | 1.60 | 1.32 | 0.99 |
| Grass model | 0.077 | 2.52 | 1.31 | 0.99 |
| Grass model | 0.055 | 3.71 | 1.31 | 1.00 |
| Grass model | 0.032 | 2.93 | 1.17 | 0.99 |
| Bamboo rod model | 0.15 | 2.18 | 1.36 | 0.99 |

Table 3. Value of parameter *a* and *b* in empirical model $I = a \cdot u^b$

### 4.1 Basic model equations

When simulating the sediment trapping process in the flume experiments with the rod model, the continuity equation (1) and the momentum conservation equation (2) were employed for calculating flows in the flume, while calculation of sediment transport used the continuity equation (3).

$$\frac{\partial B\theta h}{\partial t}+\frac{\partial Q}{\partial x}=0 \tag{1}$$

$$\frac{\partial Q}{\partial t}+\frac{\partial}{\partial x}\left(\frac{gB\theta h^2}{2}+\frac{Q^2}{B\theta h}\right)=-gB\theta h\left\{\frac{\partial z}{\partial x}+\frac{n^2Q^2}{B^2h^{10/3}}+\frac{1}{2g}NdC_d\left(\frac{Q}{B\theta h}\right)^2\right\} \tag{2}$$

$$\frac{\partial z}{\partial t}+\frac{1}{1-\lambda}\left\{\frac{\partial\sum(q_{bi})}{\partial x}+\sum(q_{sui}-w_{0i}C_i)\right\}=0 \tag{3}$$

where; $B$: flume width, $\theta$: volumetric water content in the water flowing cross section ($\theta$= 0.80 for the rod model and $\theta$= 0.85 for the grass model), $h$: flow depth, $t$: time, $Q$: flow rate, $x$: distance from the lower end of the flume, g: acceleration of gravity, $z$: flume bed level, $n$: Manning's roughness coefficient ($n$ = 0.013), $N$: number of rods per unit area, $d$: diameter of rod, $C_d$: drag coefficient of rod ($C_d$ = 2.5), $\lambda$: porosity of deposited sediment ($\lambda$= 0.42 for GK-9, $\lambda$= 0.40 for other than GK-9), $q_{bi}$: bed load transport rate per unit width of sediment in an $i$th size class, $q_{sui}$: pick-up rate of suspended load per unit area of sediment in an $i$th size class, $C_i$: sediment load concentration in an $i$th size class, and $w_{oi}$: settling velocity of sediment in an $i$th size class. $q_{bi}$ is calculated by the Meyer-Peter Müller formula, while $q_{sui}$ for the flume section is calculated by using the Itakura and Kishi formula (1980), wherein the parameter $K$ = 0.0001 (Shimada et al., 2005). On the basis of the experimental results in 3.3, $q_{sui}$ for the model section for both models is set at zero. The Rubey equation is used to calculate $w_{oi}$.

The above equations (1) and (3) are also used for experiments with the grass model, but equation (4) given below is used instead of (2) as the equation of conservation of momentum for calculating flows in the flume.

$$\frac{\partial Q}{\partial t}+\frac{\partial}{\partial x}\left(\frac{gB\theta h^2}{2}+\frac{Q^2}{B\theta h}\right)=-gB\theta h\left\{\frac{\partial z}{\partial x}+\frac{n^2Q^2}{B^2h^{10/3}}+\frac{1}{K_s^{\,2}}\left(\frac{Q}{B\theta h}\right)^2\right\} \tag{4}$$

where $K_s$ is the grass permeability coefficient (Shimizu et al., 1991). For $K_s$ ($m\cdot s^{-1}$) an empirical formula ($K_s$ = 0.0011exp(57.9·$h$)+0.313) obtained from the results of the flume experiment performed with a grass model was used, where $h$ is the water depth (m).

### 4.2 Calculation method

The numerical calculation based on the above equations used the MacCormack method (Okabe, 1992). The difference distance interval $\Delta x$ and difference time interval $\Delta t$ were set at 0.02 m and 0.005 sec, respectively. Sediment particle sizes in terms of the equivalent particle sizes were divided into four classes: 0 to 0.002, 0.002 to 0.02, 0.02 to 0.2 and 0.2 to 0.5 mm. The first two classes were used for calculations as suspended sediment while the last two were used as bed load sediment. The upstream end in the calculation was set at a point 1 to 2 m on the upstream side from the hydraulic jump location in the experiments. At this point,

the boundary conditions were set for $Q$, $h$ and $C_i$, that is, the flow rate obtained in the experiments was taken as $Q$, the normal depth of the flow condition was taken as $h$, while $C_i$ was calculated on the basis of sediment concentration and composition of particle sizes on the upstream side obtained in the experiment. The downstream end in the calculation was set at the downstream end of the flume, and the critical depth of the flow condition was given for $h$ as a boundary condition.
First, calculations used only the flow equations under the initial conditions, and at a time when the steady state condition was reached, $C_i$ was introduced at the upstream end as the sediment concentration to start the calculation. Thereafter, calculations were performed for the experiment duration for each case.

## 5. Results and discussion for numerical model simulation

### 5.1 Numerical simulation for rod model experiments

The measurements of the experiments using the bamboo rod model and the numerical simulation were compared. Figure 5 shows the measured and calculated values for the water surface and the flume bed levels in and around the rod model in the flume upon completion of the experiments on Cases A-1, A-2, A-7 and A-10. This figure indicates the calculations for the water surface and the bed level profile along the length of the flume are generally in good agreement with the experimental results. Also in terms of the water surface profile, the water level at each point including the hydraulic jump is generally simulated. Certain differences appear between the measured and calculated values of the bed level profile in the flume in the vicinity of the upstream end of the rod model. The sediment deposition depth peaks in the backwater section, while in the model section, the depth gradually becomes smaller towards the downstream end. These experimental features of sediment deposition were also simulated. The simulations also showed that the sediment concentration at the downstream end had almost no change over time.
Figure 6 indicates the comparison of the calculated and measured values for the time average of the sediment concentration at the downstream end of the flume. Calculated values of sediment concentration are similar to the experimental values, with the magnitude of relative error being 0 to 58% and mean magnitude of relative error being 23%. This shows the simulation generally reproduced the time average for the measurements of sediment concentrations obtained in each experiment.
The above comparisons suggest the numerical model established in this study can effectively simulate the sediment transport process in and around the rod model and also can estimate the time average of the concentration of sediment passing through the rod model.

### 5.2 Numerical simulation for grass model experiments

Then, the measurement results of the flume experiments with the grass model and the numerical simulation results were compared. Figure 7 shows the comparison of the calculated and measured values of the time average of the sediment concentration at the downstream end obtained in the experiments of Cases B-1 to B-6, and C-1 to C-4. Although two calculated values of B-1 and B-2 are larger than their measured values, in the other eight cases, there is good agreement between the calculated and measured values. The plotted points are above the 1:1 straight line, that is, calculated values tend to be larger than the measured values. Magnitude of relative error was in the range of 0 to 130%. More specifically, 72% and 130% for Cases B-1 and B-2, respectively, and 0 to 45% for the other cases, with the overall mean magnitude of relative error being 29%.

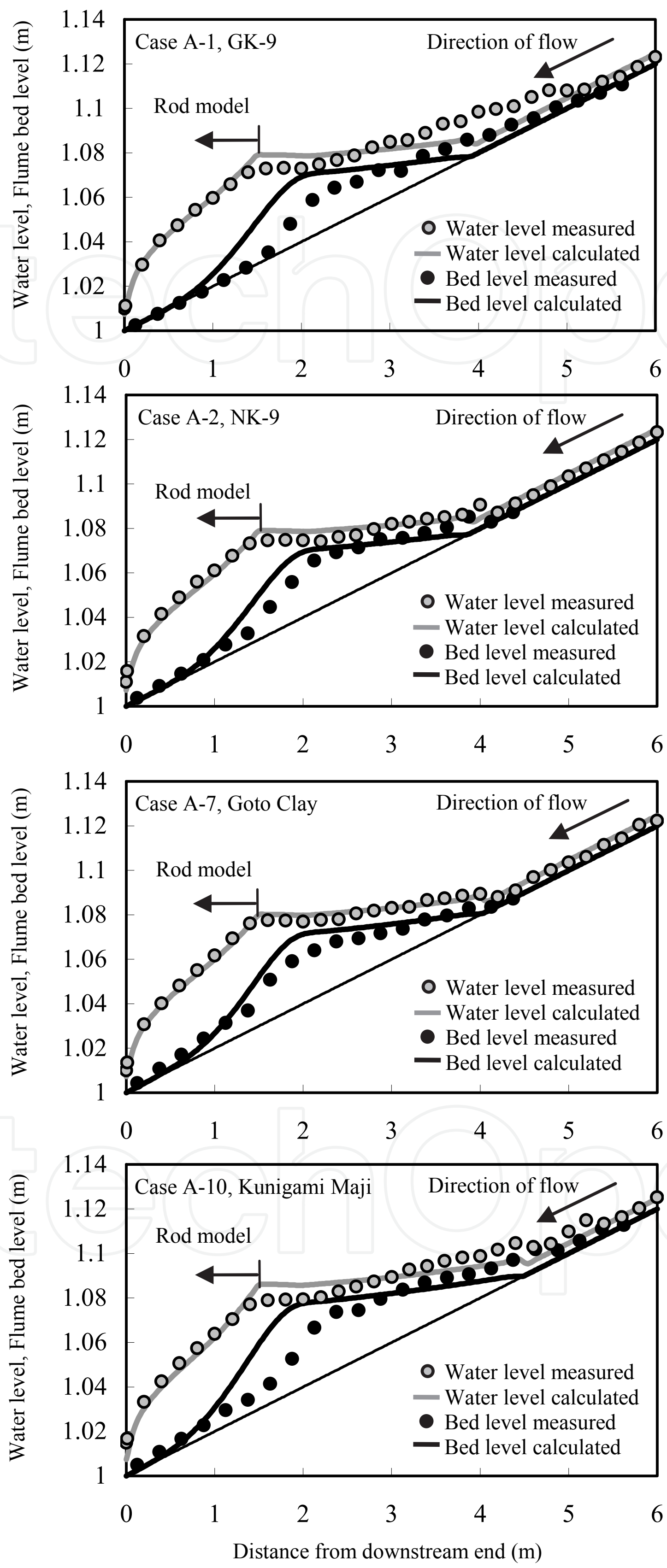


Fig. 5. Measured and calculated water and bed surface profiles in and around the rod model

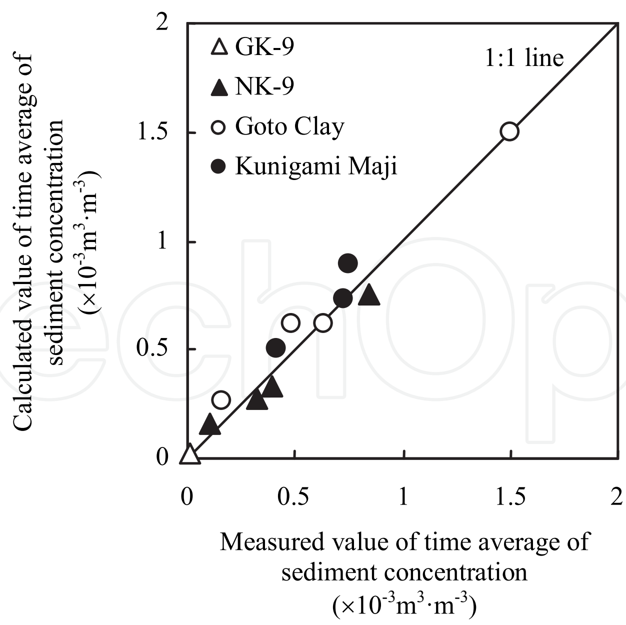


Fig. 6. Relationship between measured and calculated value of the time average of sediment concentration at the downstream end of the flume (A-1 to A-12)

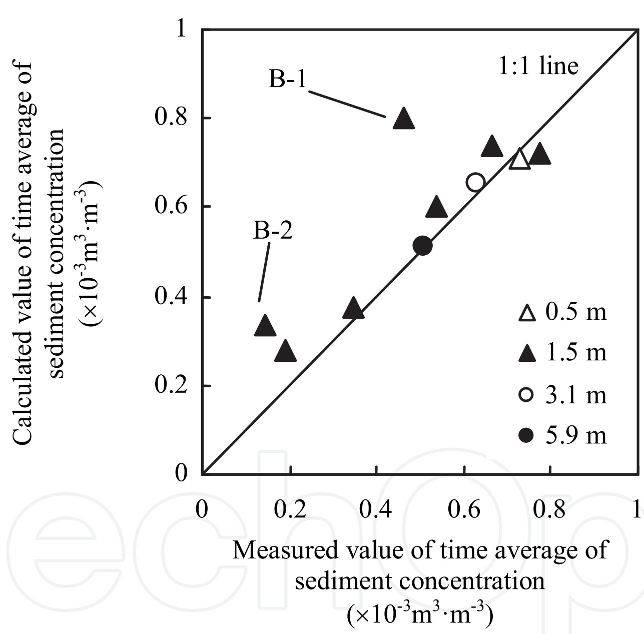


Fig. 7. Relationship between measured and calculated values of the time average of sediment concentration at the downstream end of the flume (B-1 to B-6, C-1 to C-4)

Figure 8 shows the comparison of the concentration of sediment having equivalent particle sizes of 0 to 0.002 mm, where all the calculated values are above the measured ones. The calculated values of Cases B-1, B-2 and B-4 are fairly large compared with the measured values, and in the other seven cases, the calculated values are somewhat larger than the measured ones. Magnitude of relative error was in the range of 12 to 147%. More specifically, the values were 137%, 147% and 109% for Cases B-1, B-2 and B-4, respectively, and 12 to 51% for other cases, with the overall mean magnitude of relative error being 62%.

The comparisons of the concentration of sediment having an equivalent particle size of 0.002 to 0.02 mm are given in Fig. 9. The calculated value of Case B-2 is fairly large compared with the measured value, but in the other nine cases the calculated values are similar to the measured ones. Magnitude of relative error was in the range of 3 to 124%. More specifically, the values were 124% for B-2 and 3 to 57% for the other cases, with the overall mean magnitude of relative error being 27%.

For the two equivalent particle size classes larger than 0.02 mm, all the time averages of the calculated results of $C_{out}$ were 0.00 $m^3 \cdot m^{-3}$. Comparison with the experimental results presented in 3.2 shows that the calculated values well reproduce the measured values of each experiment.

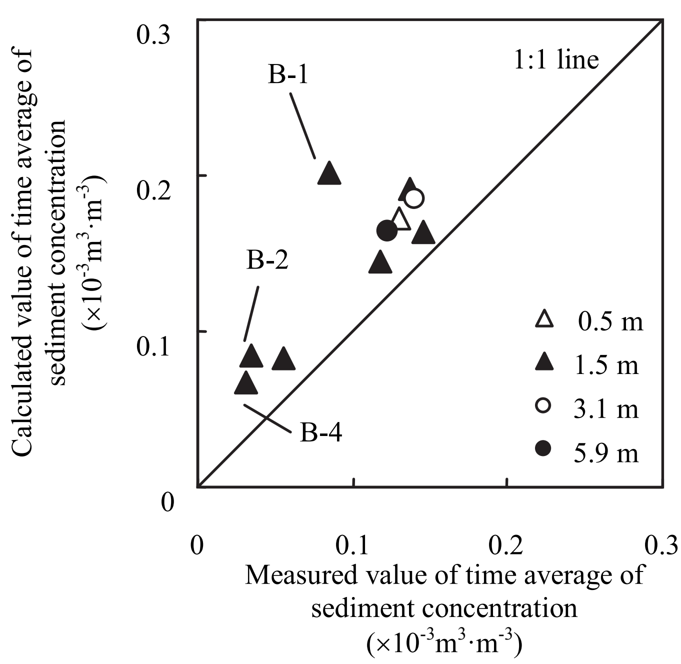


Fig. 8. Relationship between measured and calculated value of the time average of sediment concentration of 0–0.002 mm-size particles at the downstream end of the flume (B-1 to B-6, C-1 to C-4)

Comparing the time averages of the sediment concentrations for the grass model flume experiments with the numerical simulation showed good agreement for the equivalent particle size classes other than the 0 to 0.002 mm class, the calculated sediment concentration of 0 to 0.002 mm class was large. Since the ratio of the equivalent particle size class 0 to 0.002 mm was only 13% of all the sediment used in the experiments, the influence of over estimation for this size class in the model simulation does not severely affect the overall estimation. Therefore, the numerical model established in this study is valid for determining concentrations of sediment passing through the grass. The validation results indicate the model is useful to evaluate grass strips for reduction of sediment runoff.

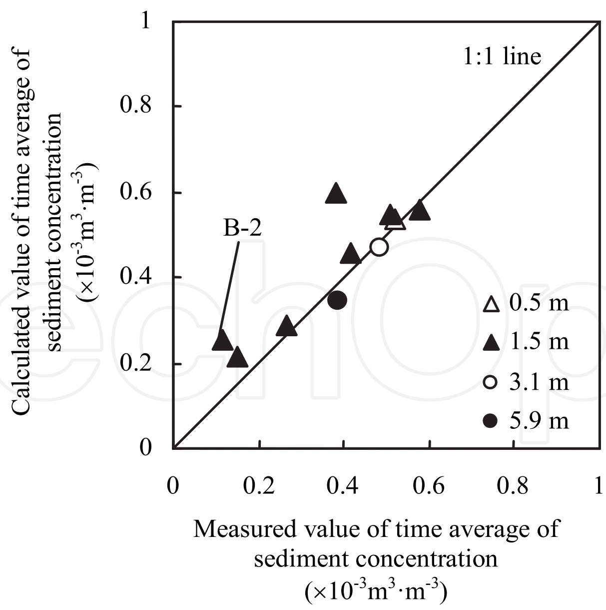


Fig. 9. Relationship between measured and calculated value of the time average of sediment concentrations of the 0.002–0.02 mm-size class at the downstream end of the flume (B-1 to B-6, C-1 to C-4)

## 6. Conclusion

This study provides an understanding of the sediment transport process in and around grass strips as part of an effort to accurately evaluate the effect of grass strips to reduce the runoff of reddish sediments to prevent runoff of reddish sediment in the Okinawa region of Japan. Based on this understanding, a mathematical model has been established to simulate the processes.

That is, flume experiments performed to simulate sediment transport in and around grass strips demonstrated (i) the features of deposition depth distribution of sediment trapped by the rod model, (ii) the relationship between the reduction ratio of runoff of reddish sediment in a grass model and the inflow rate, the length of the grass model and particle size classes, and (iii) flows in the grass are in a state of transition between laminar and turbulent flow.

Calculations from the numerical model for the rod model flume experiments verified that the model generally simulated (i) the water and the bed level profiles of the flume used in the experiments where the rod model was applied, and (ii) the concentration of sediment on the downstream side of the rod model.

Calculations with the numerical model generally simulated the concentrations of sediment for the downstream end of the grass model that were measured in the flume experiments. Although the concentration of sediment with an equivalent particle size of 0 to 0.002 mm was fairly large, the concentration of sediment with other particle sizes and the overall concentrations were in good agreement. Therefore, the numerical model established in this study can effectively estimate the concentration of sediment passing through the grass model and also the concentration of sediment of each equivalent particle size class demonstrated in this study.

Further studies are required on applicability of the numerical model under field conditions, followed by evaluation of the sediment trapping effect of grass strips with the numerical model simulation.

## 7. Acknowledgements

This study was partly granted by KAKENHI (No: 20580271). In conducting the flume experiments, Mr. Kazuya Ishizaka of the National Agricultural Research Center for Kyushu Okinawa Region offered assistance. We would like to express our sincere thanks for his efforts.

## 8. References

Dillaha, T.A., Reneau, R.B., Mostaghimi, S. and Lee, D. (1989). Vegetative Filter Strips for Agricultural Nonpoint Source Pollution Control. *Trans. ASAE,* Vol.32, No.2, pp. 513-519, ISSN 0001-2351

Haan, C.T., Barfield, B.J. & Hayes, J.C. (1994). Sediment control structures, In: *Design Hydrology and Sedimentology for Small Catchments,* Haan, C.T., Barfield, B.J. & Hayes, J.C., pp. 359-375, Academic Press, ISBN 0-12-312340-2, San Diego

Hudson, N. (1995). *Soil conservation*, Bastford, ISBN 0-7134-7353-3, London

Itakura, T. & Kishi, T. (1980). Open Channel Flow with Suspended Sediment. *Proc. ASCE,* Vol.106, No.HY8, pp. 1325-1343, ISSN 0733-9429

Minami, N., Yamada, T., Nakano, M., Tomisaka, M., Tokunaga, T. & Yamashiro O. (2002). The characteristics of red sediment discharge at different stages of cultivation of pineapple fields (in Japanese with English abstract). *J. JSECE*, Vol.54, No.5, pp. 30-38, ISSN 0286-8385

Morgan, R.P.C. (1995). *Soil erosion and conservation*, Longman, ISBN 0-582-24492-7, Essex, England

Nakasone, K., Higa, E., Mitsumoto, H. & Omija (1998). Estimation of soil loss in Okinawa prefecture (II) (in Japanese). *Ann. Rep. Okinawa Pref. Inst. Health Environ.*, No.32, pp. 67-72, ISSN 1341-0636

Nezu, I. & Tominaga, A. (2000). *Hydraulics* (in Japanese), Asakura Publishing, ISBN4-254-26139-X, Tokyo

Okabe, T. (1992). Improved model for bed-level changes in mountain rivers. *Proc. of the Int. Symposium on Erosion, Debris Flows and Environment in Mountain Regions*, pp. 139-146, ISBN 0-947571-38-8, Chengdu, China, July 1992

Osawa, K., Yamaguchi, S., Ikeda, S. & Takamuku, K. (2005). Field observation of sediment runoff reduction methods on farmland (in Japanese with English abstract). *Ann. J. Hydraul. Eng., JSCE*, No.49, p.p. 1099-1104, ISSN 0916-7374

Shimada, T., Yoshikawa, Y. & Watanabe, Y. (2005). Sediment transport in the Nibutani dam reservoir at 2003 flood of the Saru river (in Japanese with English abstract). *Ann. J. Hydraul. Eng., JSCE*, No.49, pp. 913-918, ISSN 0916-7374

Shimizu, Y., Tsujimoto, T., Nakagawa, H. & Kitamura, T. (1991). Experimental study on flow over rigid vegetation simulated by cylinders with equi-spacing (in Japanese with English abstract). *Proc. JSCE*, No.438/II-17, pp. 31-40, ISSN 0289-7806

Shiono, T., Nakamura, H., Haraguchi, N., Taruya, H. & Miyamoto T. (2005). Effectiveness of Vegetative Filter Strips for Sediment Removal under Field Conditions. *J. Agric. Meteorol.*, Vol.60, No.5, pp. 1021-1024, ISSN 0021-8588

Shiono, T., Yamamoto, N., Haraguchi, N. & Yoshinaga, A. (2007). Performance of Grass Strips for Sediment Control in Okinawa. *JARQ,* Vol.41, No.4, pp. 291-297, ISSN 0021-3551

Sugawara, K., Ohwaki, Y. & Banzai, K. (2001). Erosion Control in Pineapple Fields on the Island of Ishigaki. *JARQ*, Vol.35, No.2, pp. 91-96, ISSN 0021-3551

Yoshinaga, A. & Onaga, K. (1993). Suspended soil from reclaimed farmland of Kunigami-Maji area in Okinawa (in Japanese with English abstract). *Trans. JSIDRE*, No.168, pp. 105-110, ISSN 0387-2335

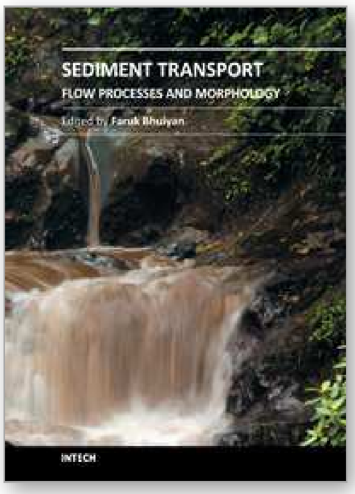


**Sediment Transport - Flow and Morphological Processes**

Edited by Prof. Faruk Bhuiyan

ISBN 978-953-307-374-3
Hard cover, 250 pages
**Publisher** InTech
**Published online** 26, October, 2011
**Published in print edition** October, 2011

The purpose of this book is to put together recent developments on sediment transport and morphological processes. There are twelve chapters in this book contributed by different authors who are currently involved in relevant research. First three chapters provide information on basic and advanced flow mechanisms including turbulence and movement of particles in water. Examples of computational procedures for sediment transport and morphological changes are given in the next five chapters. These include empirical predictions and numerical computations. Chapters nine and ten present some insights on environmental concerns with sediment transport. Last two contributions deal with two large-scale case studies related to changes in the transport and provenance of glacial marine sediments, and processes involving land slides.